



Effects of species and moisture content on the behaviour of solid wood under impact

Mojtaba Hassan Vand¹ · Jan Tippner¹ · Martin Brabec¹

Received: 2 December 2022 / Accepted: 22 August 2023 / Published online: 19 September 2023
© The Author(s) 2023

Abstract

The article's main aim is to assess the effects of species and moisture content (MC) on the behaviour of solid wood material under the low velocity of impact and present a pattern for predicting loading vs time curves for these species in different moisture levels. Three groups of samples (300×20×20 mm) were made from beech, oak, and spruce wood. Each group was subdivided into two groups with low moisture content (LMC) level (10–12%) and high moisture content (HMC) level (40–60%). A drop-weight impact machine did the tests, and high-speed cameras recorded the lateral specimens' surface during the impact. The digital image correlation technique (DIC) determined the strain pattern and the deflection. The timing of the crack initiation was also observed. Also, the force–time charts, the maximum force required for crack initiation, the work needed for crack initiation, and the total work required for the breakage of every specimen were gathered. A general force–time pattern with five identifiable steps was determined for each group. It turned out that the maximum deflection and longitudinal tensile strain of the beams up to crack initiation increase with increased moisture content while maximum force decreases. Unlike beech, the required work for rupture of HMC samples of oak and spruce is higher than LMC group.

1 Introduction

Jansson (1992) did a series of static and impact tests to conclude the failure modes and failure stresses. The strength ratio between dynamic and static failure stress (with different loading rates) was measured to clarify the effect of impact loading. The research stated that both the initiation and propagation toughness increase with the loading rate. Bocchio et al. (2001) compared the static and impact bending strength of two species, and they showed that the species effectively determines the wood behaviour (in their research, the guard-rail for the roads), and brittleness or the ductility of the species may be a vital property. Jacques et al. (2014) tested lumber within a range of low and high strain rates to study the influence of loading rate on the flexural response of typical light-frame wood construction. A single-degree-of-freedom iterative solution procedure computed the modulus of rupture (MOR) and modulus of elasticity (MOE). Marur

et al. (1994) offered a simple dimensional inertial model for transient response analysis of isotropic homogenous notched beams under impact. Their mass-spring model was able to model the impact process despite the simple linear nature of the formulation. Wood (1951) offered a mathematical expression of the relationship between an important structural property of wood, such as bending strength and load duration. An empirical hyperbolic equation is developed to represent the data trends using the data of small clear beams subjected to long-time, rapid, and impact loading. Found and Howard (1998) developed a mathematical spring-mass model to describe the drop-weight impact response of CFRP panels. The presented model can identify the different influences of the main impact impulse, high-frequency oscillations, and free vibrations on the force–time plot of the impact. Also, this model can distinguish the difference in response in thin and thick laminates. It can be used as a reliable guide for effective digital filtering of signals from drop-weight impact tests. Xing et al. (2013) studied dynamic fracture behaviour using a three-point bending drop-weight test method to clarify the effect of impact velocity on the impact behaviour of the samples. Olmedo et al. (2015) measured the dynamic response of fresh stems under impact loading experiments using Charpy's test. They offered a practical method for assessing the capacity of wood structures, which

✉ Mojtaba Hassan Vand
xhassanv@mendelu.cz

Martin Brabec
martin.brabec@mendelu.cz

¹ Mendel University, Brno, Czech Republic

considers the inertial effects of the impacts. In order to overcome the difficulties in interpreting the resulting data due to a lack of a detailed understanding of the inertial forces and the wave mechanics in Charpy's specimens, Yokoyama and Kishida (1989) proposed using the Split-Hopkinson pressure-bar technique for the three-point bending impact test. They concluded that a reliable result could only be obtained by evaluation procedures considering the inertial effects. Rubio et al. (2003) studied the dynamic fracture-initiation toughness of materials by doing three-point bending tests using a Split Hopkinson Bar. A high-speed photography system measured the crack and crack mouth opening displacement propagation. Jiang et al. (2004) performed dynamic three-point bending tests with a Hopkinson pressure bar. They tested the pre-cracked three-point bending specimen to derive a formula for the dynamic stress intensity factor. They used the vibration analysis method considering shear deformation and rotary inertia, which influence the stiffness and the natural frequency. Widmann and Steiger (2009) experimentally studied the impact bending and static bending behaviour of large-sized samples of Norway spruce wood with a 3-point bending test without consideration of inertia effects. The impact bending strength and work were significantly higher (about 27% in bending strength) than static ones. Polocoşer et al. (2016) compared the energy absorbed by samples loaded by static three-point bending and dynamic pendulum tests. Polocoşer et al. (2018) studied the dynamic failure stresses and stiffness of three different wood species subjected to low-velocity impact testing. They validated the analytical computations based on Euler–Bernoulli and Timoshenko beam theories in combination with a plastic contact law. Fortin-Smith et al. (2016) performed a two-step method to characterize the mechanical behaviour of wood. In the first step, a four-point bending test was done to determine elastic moduli and strength. Also, Charpy's tests determined strain at failure as a function of strain rate and wood density. In the next step, finite element simulation using the experimental data was performed. Yamada et al. (2018) determined the energy absorbed by the shelter facilities by measuring the projectile's velocity before and after the impact. Baumann et al. (2021) used an impact pendulum test setup to investigate the effect of the temperature at five temperature levels, ranging from -30 to $+90$ °C, on birch and beech wood impact behaviour.

Many researchers tried different approaches to express the relationship between an important structural property of wood, such as bending strength, and the load duration for the structural engineers designing a load-bearing part of a shock absorber in the road industry. The three-point bending (TPB) test has become an essential tool in determining the mechanical behaviour of a material under high-rate loading and impact (Marur et al. 1994). It can be used to assess different types of isotropic or orthotropic materials, such as

composites, for evaluating the effects of material properties, geometric dimensions and type of loading (Daniel et al. 2002). In the processing and measurement of static fracture toughness, two parameters of length and force are involved. However, measuring dynamic fracture toughness data requires additional parameters, and time is the most critical parameter to consider. Also, the influences of time on material behaviour must be measured. However, the time parameter can also influence the measuring procedure (Kalthoff 1985). Fracture energy cannot be specified in terms of force and dimension alone. It also depends on the rate at which it is supplied to the fracture process, regardless of whether the internal material structure is isotropic or orthotropic (Guo et al. 1997). In general, dynamic measuring procedures have their roots in measuring procedures for equivalent static values. Static procedures are often transferred directly to dynamic ones without changes or slight modifications (Kalthoff 1985). Ideally, the impact test should be designed to simulate the loading conditions and reproduce the failure modes and mechanisms likely to occur on a component in operational service or natural environments, such as low-velocity impact by a large mass (such as boulders) and high-velocity impact by a small mass (such as runway debris, small arms fire). These tests are generally chosen based on the desired condition to simulate, such as drop-weight or a swinging pendulum for lower and higher velocities, a gas gun, or some other ballistic launcher (Cantwell and Morton 1991). Since the methods and standards are different in testing dynamic loadings, there are differences between the results, making direct comparisons of the dynamic response complicated (Found and Howard 1998). Also, while standard test methods and specimen geometries permit comparisons between the impact response of different materials, extreme care should be used to predict the likely response of large structures based on small laboratory specimens (Found and Howard 1998). Based on some research done, it can be stated that the damage initiation and growth are closely dependent on both impact source properties (e.g., impact force, impact velocity, impact energy) and impact response of the material (e.g., material strength, displacement under force, energy dissipation, impact duration). Even the shape of the impactor, length-to-diameter ratio, and impactor's mass are among the parameters that have a crucial influence on damage characteristics (Evcı and Gülgeç 2012).

The relation of wood's strength to the load's duration has been investigated at laboratories for many years. However, despite the considerable amount of time and effort, the lack of accurate experimental tools with the ability to observe the test specimens during the test causes a need to redo some tests to re-evaluate the results of impact tests (Wood 1951). Although the inelastic strains produced by dynamic loads have been investigated extensively, the dynamic failure of structures due to severe deformations and material rupture

is poorly understood. The main difficulty lies in the fact that deformation is a global response, while failure is a local phenomenon (Yu and Jones 1997). Measuring the absorbed loading at the time of impact is a means of assessing the deformation properties of the test sample. One of the main issues is the locality of the deformation in that the evolution of localized damage zone is the main region of the rupture in heterogeneous materials (Hao et al. 2010). However, the effect of the strain locality can be overcome by determining the strain pattern and deflection in a full-field mode. The effect of species on the impact behavior of wood should also be considered (Lokaj and Vavrušová, 2010). The displacements and deformation of test samples are possible by using a high-speed camera which captures the lateral sample's side during the test and using the camera images as an input for the digital image correlation (DIC) technique (Yamada et al. 2018).

DIC is a robust optical method for displacement measurement and strain calculation based on image processing. A typical experimental arrangement for DIC consists of an incoherent light source to illuminate the object's surface uniformly, and a digital camera suitable for the loading rate of the test is placed parallel to the illuminated surface (Zhang and Arola 2004). DIC can process the data in a full-field mode and can be used to evaluate the more critical points, such as joints (Timbolmas et al. 2022). According to Haldar et al. (2011), DIC has immense potential within wood mechanics, especially in fracture studies. However, it should be noted that DIC also has excellent potential for other biomaterials due to its advantages (Gómez et al. 2021). However, appropriate DIC requires a high-contrast texture of captured surface with a random grey intensity distribution, i.e., a specific speckle pattern with a constant grey level during the test. Creating this speckled pattern can be challenging to fulfil when (besides others) the soaked specimens are loaded and captured, as in this study, the leaking water changes a grey intensity significantly and washes the pattern, thus, making recognizing tracking points difficult or impossible. However, the soaked wood has almost sufficient contrast and does not need an artificial speckle pattern. For non-contrast wood species, a slurry of talcum powder can fill the lumen and consequently provide the required greyscale and enhance the quality of images to an acceptable level (Thuvander et al. 2000). The undesired changes in grey levels caused by leaking water can be considerably overcome using incremental correlation when matching the tracked pixels (Pan et al. 2009). There are articles about applying DIC in tensional, compressional high-rate wood loadings; however, the analysis of wood samples under 3-point bending impact loading is missing (Dave et al. 2018). This study aspires to fulfil this lack. In order to verify the hypothesis about the different impact behaviour of various wood species, this study

collects accurate data about the force and deflection pattern of wood under high-rate bending loading.

The main aim of this article consists of a few connected objects. The effect of the species on the mechanical properties of wood in static loadings and the severity and patterns of the effect of the species has been studied and evaluated (Glass et al. 2010). However, the correspondence of the species on the mechanical properties in dynamic loadings needs to be studied more extensively. The first main objective is to evaluate the species' effect on the wood's impact behaviour by comparing the results of the tests of three different species. The second object is the determination of the effect of the moisture content. The moisture content level can affect the dynamic behaviour of wood (Hernández et al. 2014). The effect of the moisture content can be derived by creating groups of samples from the same species but with different moisture content.

2 Methodology

2.1 Production and preparation of the samples

Solid wood boards of European beech (*Fagus sylvatica* L.), English oak (*Quercus robur* L.), and Norway spruce (*Picea abies* L. Karst) were provided by a local sawmill processing the wood from stands close to Brno. The test specimens were made from these boards as clear special orthotropic blocks with the dimensions of 300 × 20 × 20 mm (longitudinal × radial × tangential direction). In total, 90 specimens were made for each species in a way that 30 specimens were stored in an environment of 20 °C and 65% relative humidity up to the equilibrium moisture content (EMC) of $11 \pm 2\%$; these groups are called the low moisture content group (LMC). The moisture content was determined gravimetrically as a difference in the weight of the specimens just before the impact test and after drying to oven-dry state related to oven-dry weight. The other 60 specimens were submerged in water to increase their moisture content level and were called the high moisture content groups (HMC). The moisture content of the second group had a broader spectrum; however, the Kruskal–Wallis test and post-hoc Tuckey's test proved almost in all cases no effect of MC on investigated parameters of the higher moisture level group (P -value $< < 0.001$); therefore, the HMC group was considered one group, and it was not necessary to be divided into more groups. Median EMC of beech, oak and spruce for HMC was 56%, 49% and 56%, respectively. The thin uniform white paint coating and black speckle pattern were created on the lateral LMC specimens' side to be captured. The texture of HMC specimens has sufficient contrast and does not need an artificial speckle pattern.

2.2 Impact tests configuration

The tests were done in the Mendel University research centre laboratory in Brno Utechov, Czech Republic. The test was carried out on the drop-weight impact testing machine DPfest 400 (Labortech s.r.o., CZ). The impact test was performed according to CSN 490115 (1979) and CSN 490117 (1980) as the three-point bending test with a 9.05 kg hammer dropped from the starting height of 815.7 mm. This configuration resulted in a 72.4 J potential hammer energy and the velocity of the hammer at the impact equal to $4 \text{ m}\cdot\text{s}^{-1}$. The position of the hammer was controlled with 0.01 mm readability, and the reaction force was sampled with a frequency of 1 MHz by the HBM force sensor CFTplus series installed on the hammer. The tests were done at room temperature ($\approx 20 \text{ }^\circ\text{C}$). Half of the specimens from each group were tested in the radial direction and the other half in the tangential direction to investigate the grain direction's effect on the impact strength and other determined parameters.

2.3 DIC equipment utilization

The strain pattern on the lateral side of specimens and deflection of specimens was determined by employing a digital image correlation (DIC) technique in a $2 \times 2\text{D}$ configuration. An acquisition set consisted of two independent high-speed (HS) cameras. One was Photron Fastcam SA-X2 1000 K-M2 with a cell size of $20 \mu\text{m}$ equipped with a lens Nikon Micro-Nikkor G with a focal length of 105 mm and two teleconverters Nikon. In contrast, the latter was Olympus i-SPEED 726R with a cell size of $13.5 \mu\text{m}$ equipped with a lens Nikon Macro-Nikkor with a focal length of 200 mm. Both cameras were positioned horizontally to align the specimens' length direction with the longer side of the field of view and, simultaneously, planned parallel to the specimens' surface to be captured. The lower resolution ($1024 \times 672 \text{ Px}$) camera (Photron) was used for the detailed study of the middle-third part of the specimens; whereas, the higher resolution ($2048 \times 600 \text{ Px}$) camera (Olympus) for the study of the whole lateral specimens' surface (Fig. 1). Both cameras took the images with 20,000 fps rate. Two high-speed MultiLED QT light sources enhanced the texture contrast on the captured surface. The images were processed in Vic-2D v. 2010 (Correlated Solutions, Inc.). The conversion factor was obtained by using a simple scale calibration. The strain tensor was computed using the Lagrange notation. The lowest possible displacement field of 3×3 points and the strain filter size of 5×5 points were applied to obtain a high strain resolution. For the LMC specimens, the standard correlation with the same reference image (the first image) for all other images was sufficient; meanwhile, for HMC specimens, the incremental correlation with changing reference (the previous image) for all other images had to be applied.



Fig. 1 Acquisition set of two independent high-speed cameras used for capturing the lateral specimens' surface during the impact test

3 Results and discussion

Figures 2, 3, 4, 5 show the average deflection of specimens for each group. As evident, the loading direction has almost no effect on the deflection pattern. However, the MC has an apparent effect on the deflection.

DIC can give a considerable amount of data, and generally, it has magnificent potential for analysis of the failure process. Figures 6, 7, and 8 show the strain distribution in 3 steps before the crack initiation, further at the moment of cracking, and after failure. Despite of unique potential of the DIC, there are some defects and limitations to the impact bending test. The area near the hammer cannot be processed due to considerable local compression, causing the disappearance of points adjacent to the hammer. However, this local compression basically does not result in the failure of specimens, and failure always starts at the lower specimens' surface due to the exceeding tensile strength. The lack of ability to match the points after cracking (Fig. 8) and losing the output's accuracy is considered the more pronounced limitation of DIC. Thus, it is better to use DIC up to breakage and neglect the data after crack initiation due to a high risk of mistakes. For HMC specimens, the matching ability was reduced by leaking water drops due to the shock of the impact. However, measuring without contacting the sample and expressing the locality of the strain field is the priority that DIC can accomplish efficiently. By considering the location of the crack initiation, the location of the maximum longitudinal strain can be derived. Figure 9 illustrates the longitudinal strain of the beam at the moment when the crack was initiated. The maximum strain magnitude was not affected by the loading direction; however, the MC affected the maximum strain.

Figure 10 shows the average force–time pattern of all specimens within the groups. It should be stated that $\sim 10\%$ of the specimens showed abnormal behaviours; thus, their

Fig. 2 Deflection of beech specimens with high and low moisture content

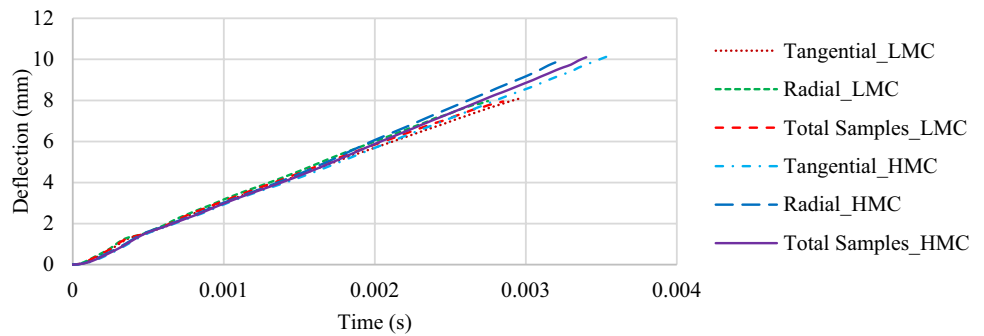


Fig. 3 Deflection of oak specimens with high and low moisture content

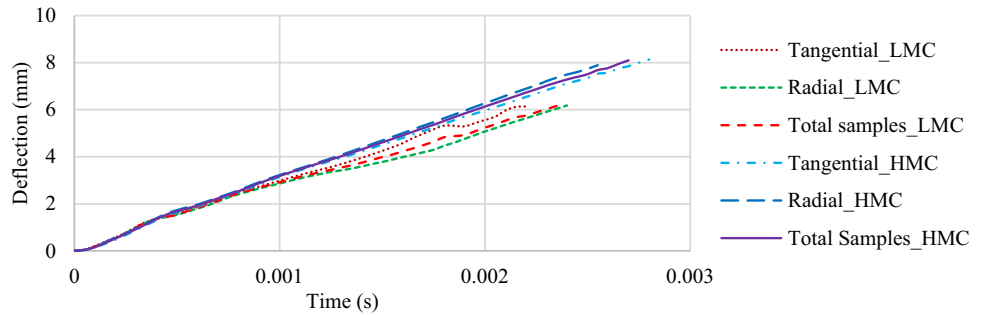


Fig. 4 Deflection of spruce specimens with high and low moisture content

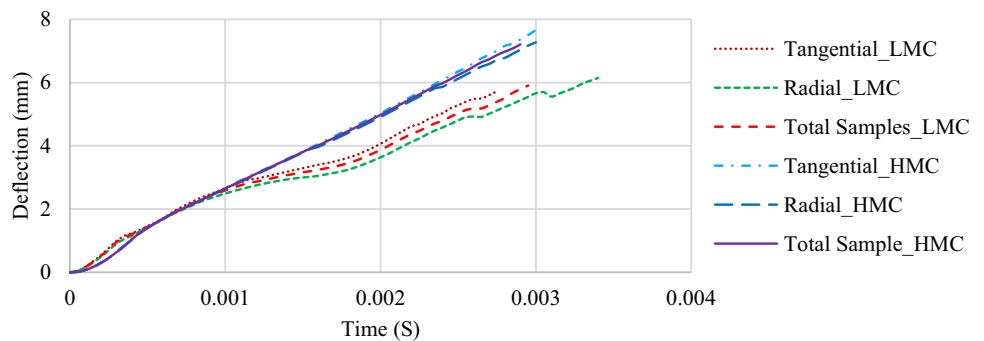
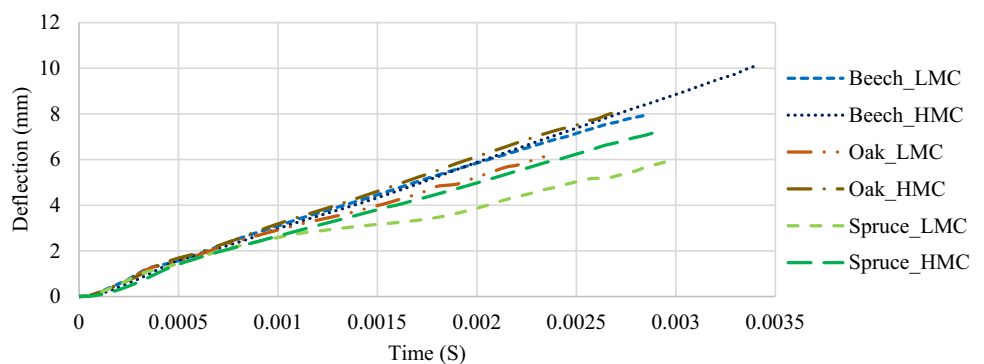


Fig. 5 Comparison of deflection for all species with different moisture content



corresponding charts were cut out of the results. These abnormalities may occur due to knots or defects hiding inside the specimens and may not be recognized by the naked eye inspection.

In general, it can be recognized that the force–time pattern has five steps. These steps may vary in size or location; however, their presence is inevitable. Figure 11 shows these steps as follows:

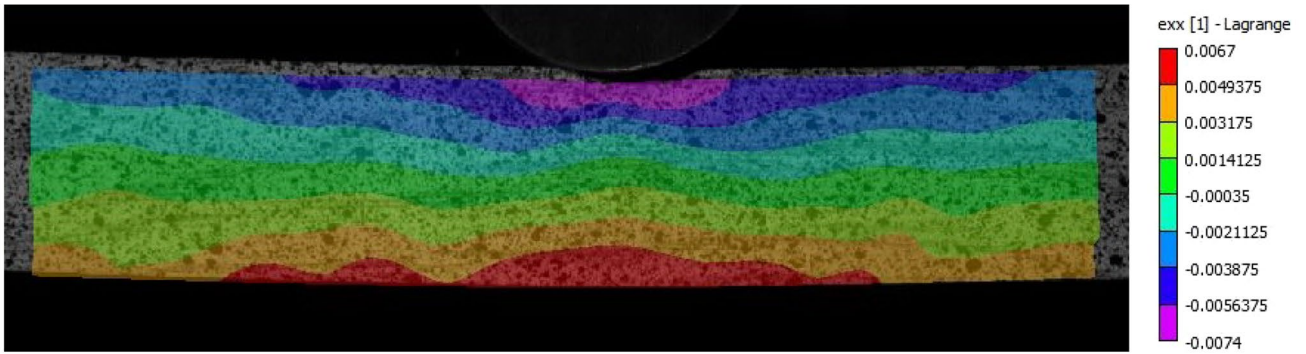


Fig. 6 Axial (longitudinal) strain during bending before any sign of crack

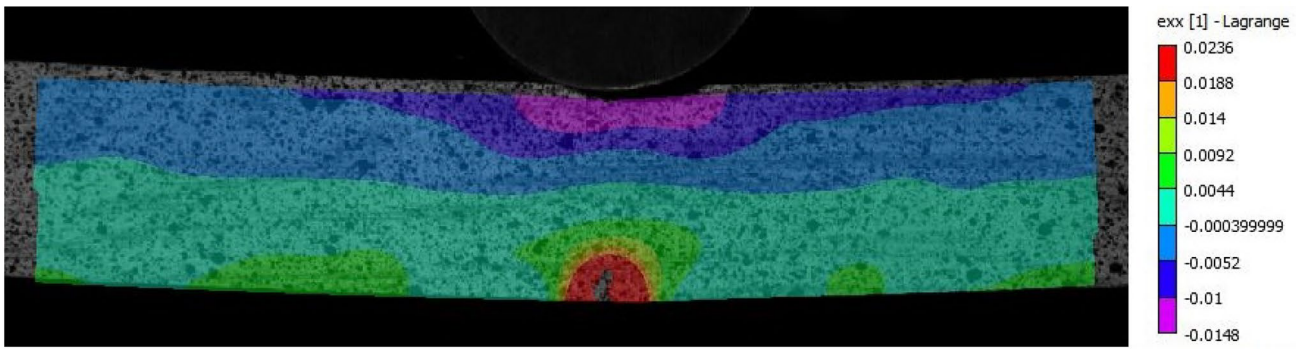


Fig. 7 Axial (longitudinal) strain at the moment of crack initiation

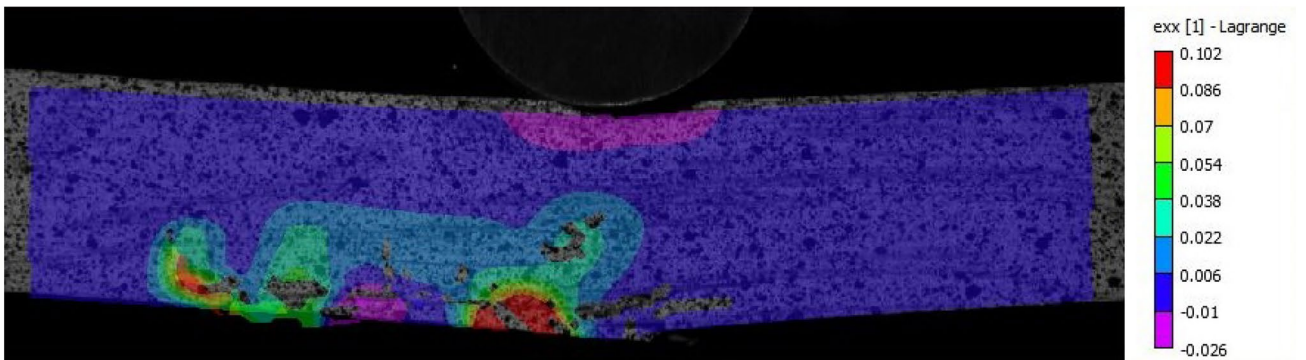
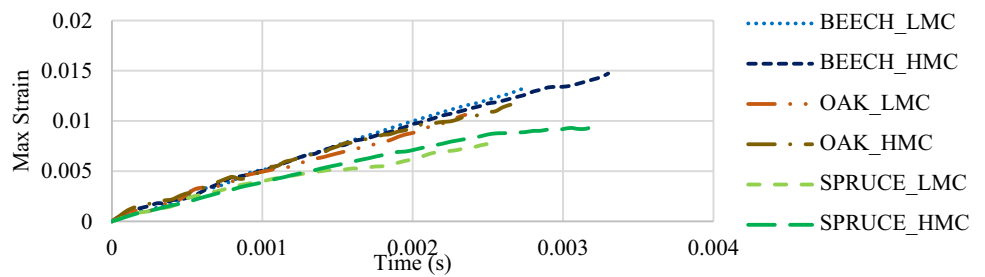


Fig. 8 Axial (longitudinal) strain during the cracking up to total breakage

Fig. 9 Maximum strain up to crack in all three species at low and high moisture content



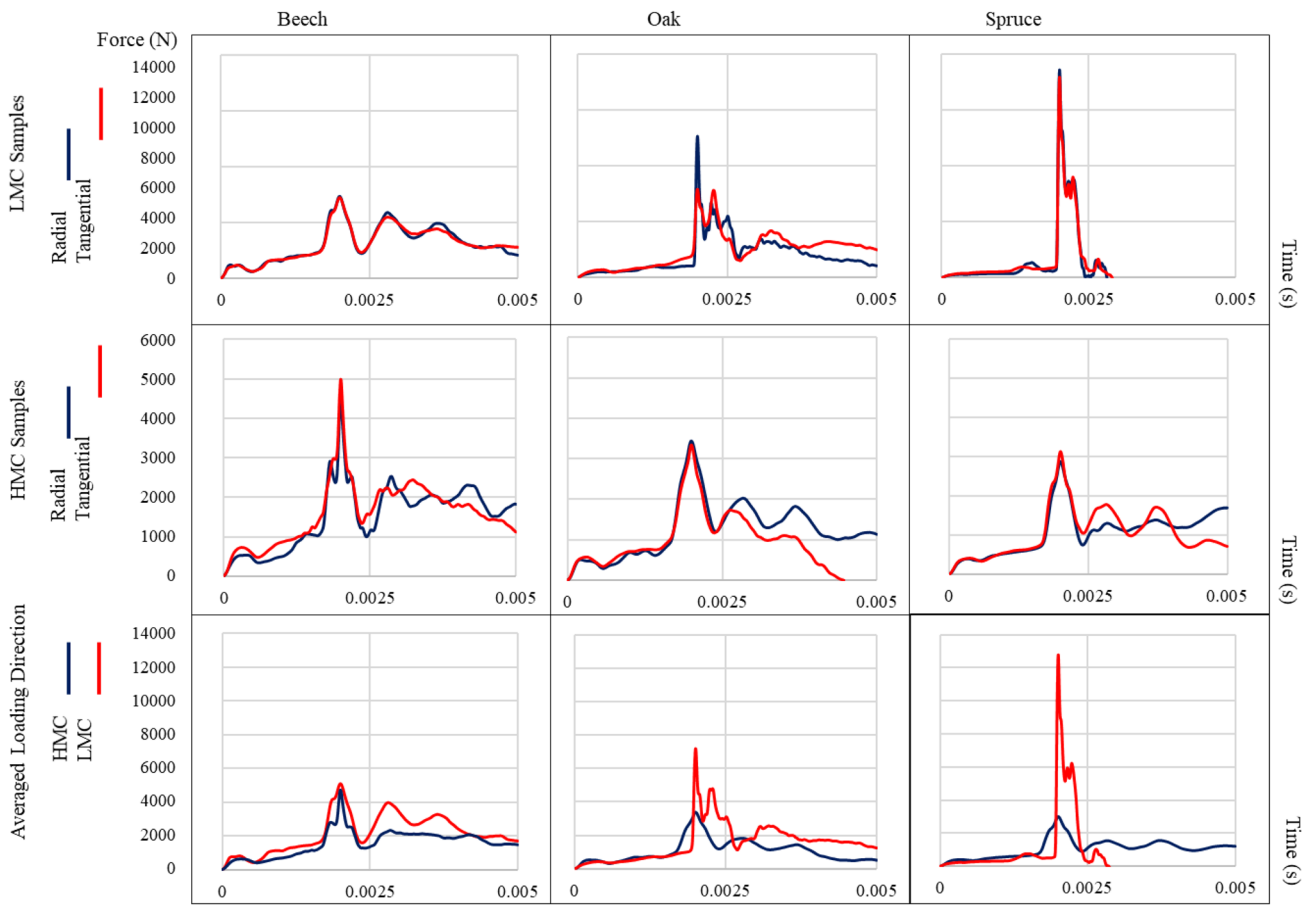
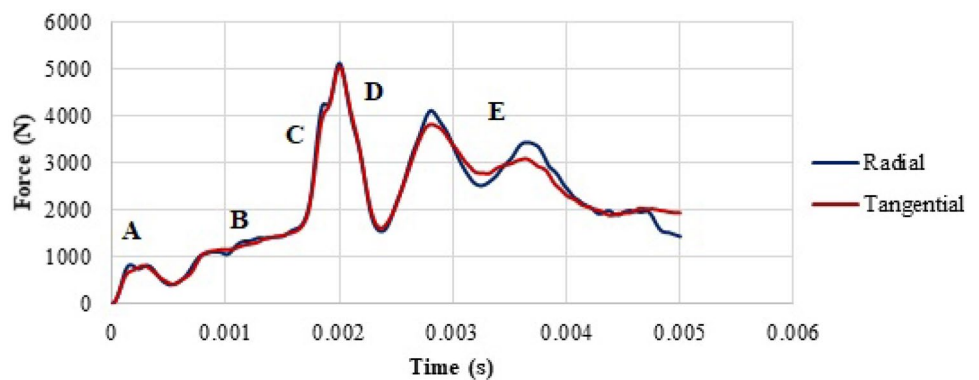


Fig. 10 Force–time curve (pattern) of HMC and LMC beech, oak, and spruce loaded in radial and tangential direction

Fig. 11 Force–time curve (pattern) of beech specimens with low moisture content under tangential and radial impact



- A. Some researchers call the first small peak the inertial peak (Marsavina et al. 2010).The inertial contribution is predominant at the early impact stage because the specimens' deflection remains small. This contribution soon decreases and almost vanishes. This small local peak is always followed by a small local trough, resulting from a slight detachment of the specimen from the hammer due to initial inertia.
- B. The gradual increase of force with slight oscillations. At this stage, the specimens loaded in a radial direction slightly have more vibration than tangentially loaded specimens. It should be taken into consideration that steps A and B are not significantly distinguishable for spruce.

- C. Sudden and almost stable increase of force up to the maximum force. At the maximum point, the crack is initiated.
- D. Sudden considerable decrease of force after initiation of crack.
- E. Random vibration from initiation of crack up to total failure. At this stage, the crack gradually increases, and the specimen gradually breaks.

The loading direction does not affect the force–time pattern of all specimen groups. Also, that beech behaviour is far less affected by the MC, unlike oak and spruce, which are more affected by the moisture content. An increase in the MC decreases the maximum force and smooths the force–time pattern. To determine these patterns, it must be clarified that the shapes of the patterns of samples were similar; however, the location of the peaks and troughs of each sample usually was different. This difference in location neutralizes the effect of peaks and troughs, so it was necessary to shift the peaks and troughs in a way that creates an understandable shape. This situation forced us to shift all the global maximum of each chart to one point, and by doing this shift, some charts were compressed or stretched. This change did not affect the general shape of the

pattern; it just affected the total length in the x-axis (time) in a way that a final shape was created. Another parameter is the impact force achieved when the mid-span displacement reaches its maximum. This force value, not affected by the early contact oscillations, provides information concerning the impact force at the transition from the loading to the unloading phase (Olmedo et al. 2015).

The wood species and MC effect were quantified by calculating the median of impact test parameters. Figures 12, 13, 14, 15, 16, 17, 18 show the maximum deflection, maximum force, the work required for crack initiation, and total work required for rupture. The differences were statistically evaluated, proving that MC affects the parameters such as work, maximum deflection, or maximum force for all wood species.

Based on Figs. 12 and 13, it can be seen that for all species, maximum deflection increases with an increase in MC. All species had a ~20% increase in max deflection by increasing their MC from ~11% to 40–60%. However, the orientation of growth rings does not significantly influence the maximum deflection. Both radial and tangential directions reach the same deflection before the crack initiation and the orientation of growth rings can cause a change from 3% up to a maximum of 7%; thus, the effect of the orientation of

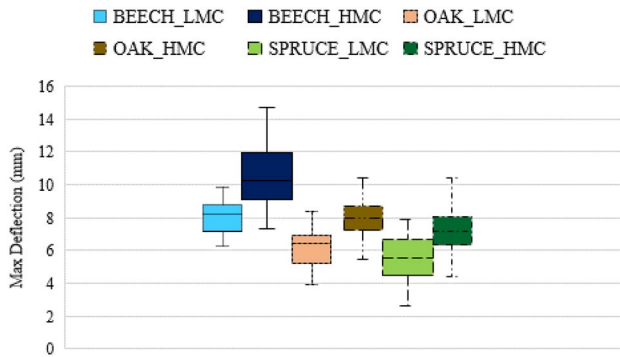


Fig. 12 Maximum deflection of each species in low and high moisture content level

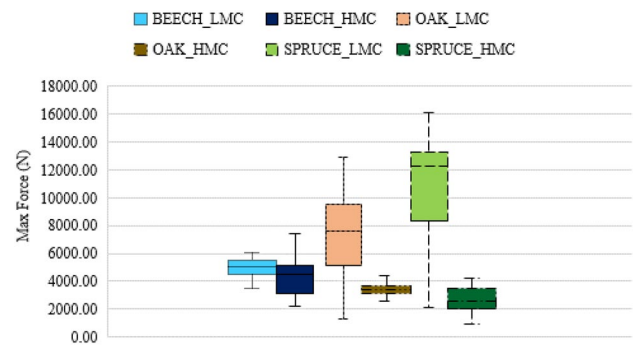
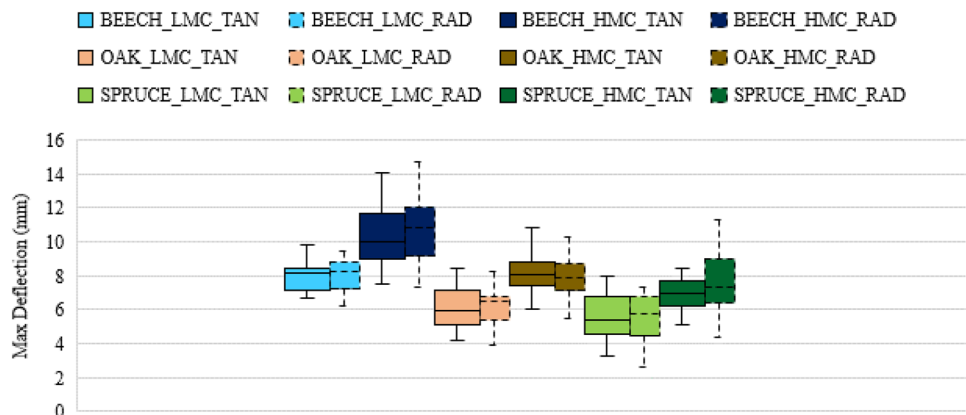


Fig. 14 Maximum force (force required for crack initiation) of each species in low and high moisture content level

Fig. 13 Maximum deflection of each species in low and high moisture content levels and loading direction



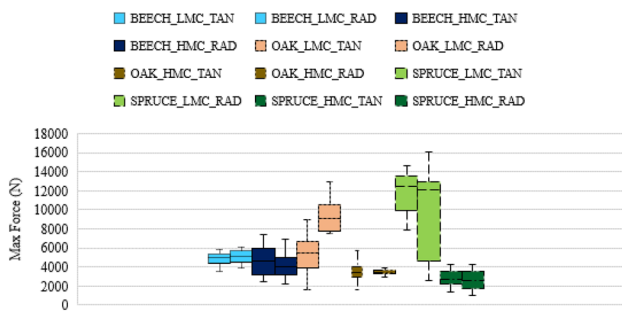


Fig. 15 Maximum force (force required for crack initiation) of each species in low and high moisture content levels and loading direction

growth rings relatively is not significant. Last but not least, for both LMC and HMC groups, beech can reach to more extended deflection, and spruce has the slightest deflection. The LMC species groups had 30 test samples; each radial and tangential orientation had 15 pieces. For HMC groups, each radial and tangential group had 30 pieces, making 60 samples for each HMC group. However, the number of samples may change slightly due to technical limits.

Figures 14 and 15 illustrate the maximum force for crack initiation. It can be seen from Fig. 14 that for all species, with an increase in MC, the maximum force decreases. The decrease of the maximum force median is 11%, 55% and 80% for beech, oak and spruce species, respectively. Figure 15 states that the orientation of loading is not significantly effective for most groups. Also, it can be seen that for LMC groups, the max force for crack initiation of beech samples is the least, and the spruce needs the highest force for cracking in a way that this value is 5000, 7500 and 12,200 (N) for beech, oak and spruce respectively. However, for the HMC groups, the trend is opposite with lower severity of difference. Figure 15 shows that all groups except oak LMC show no significant difference in the maximum force required for cracking in different orientations.

Fig. 16 Work required for crack initiation (work done up to maximum force peak) of each species in low and high moisture content level

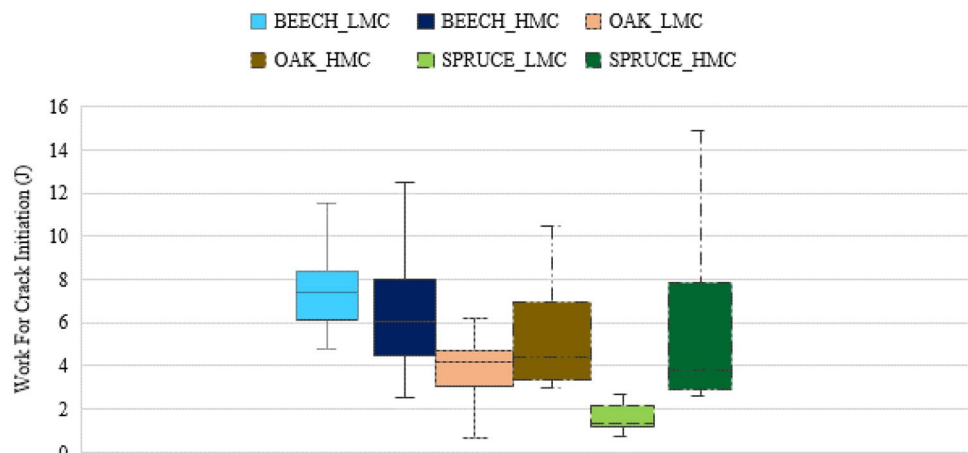


Figure 16 represents the required work for crack initiation. The median of required work for crack initiation is less for beech HMC than for LMC specimens; however, HMC specimens of spruce and oak require more work for crack initiation.

Figures 17 and 18 represent the required work for rupture. By using impact bending strength (IBS) instead of the work itself, we can avoid the effect of the dimensions up to a point making the comparison easier. IBS is the ratio of the required work for rupture (J) divided by the rectangular surface of the sample (cm²) (Gaff et al. 2018). The median of IBS of beech 7% decreases by increasing MC, while IBS of oak and spruce increase by 15% and 86% respectively. One of the parameters that can be found in the former research is IBS for rupture and due to MC, only LMC group can be compared. The IBS for beech has the least difference compared to other studies, with only 1%, 13% and 22% difference from Lokaj and Vavrušová (2010), Kubojima, et al. (2000) and Borůvka et al. (2018). However, for oak and spruce our results showed a high difference with the other research results. IBS for oak samples was almost half of other results (Gaff et al. 2019, LOKAJ and VAVRUŠOVÁ, 2010) and spruce samples showed IBS which was 30% of the former studies (Gaff et al. 2019, LOKAJ and VAVRUŠOVÁ,

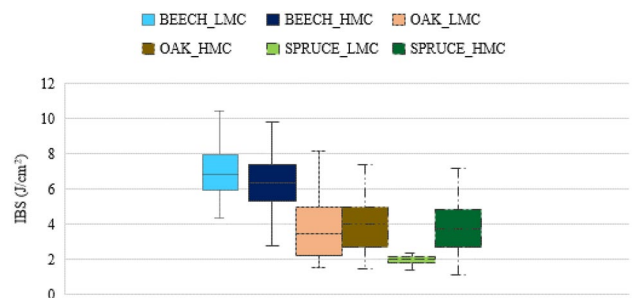


Fig. 17 IBS for specimens' failure of each species in low and high moisture content level

Fig. 18 IBS for specimens' failure in low and high moisture content levels and loading direction

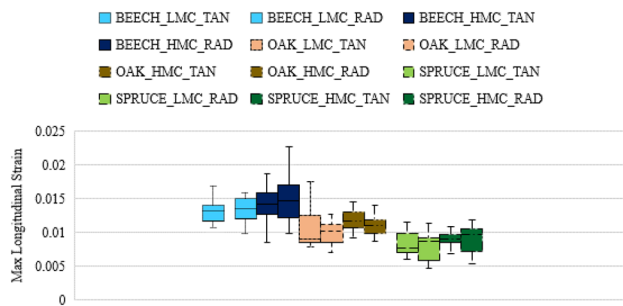
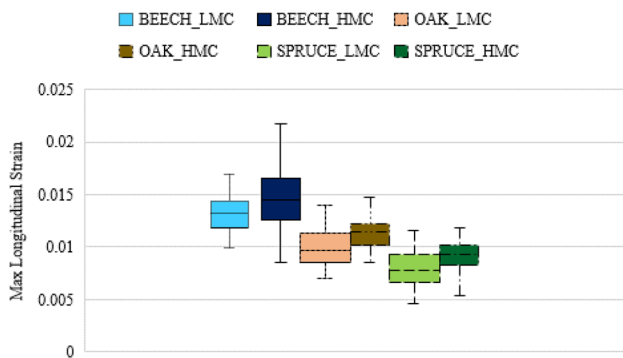
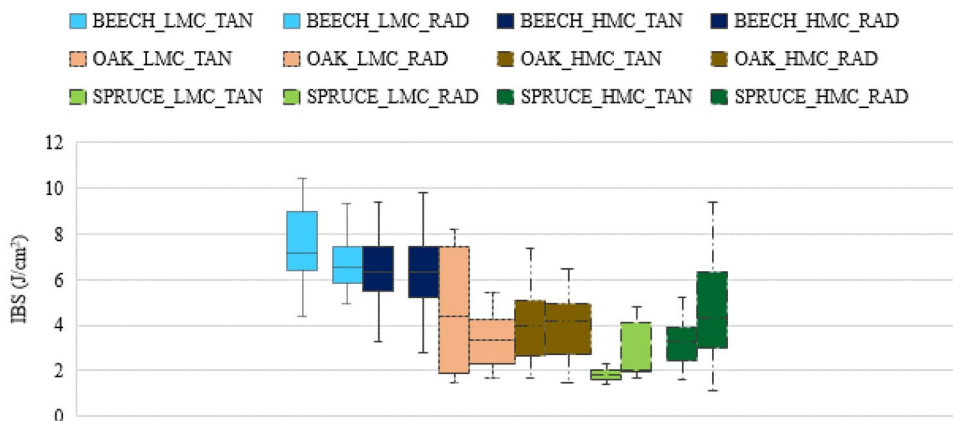


Fig. 19 Maximum longitudinal strain of each species in low and high moisture content level

Fig. 20 Maximum longitudinal strain of each species in low and high moisture content levels and loading direction

2010). These considerable difference can be due to difference in computation method of work based on the type of the test. The beech HMC specimens have less IBS than LMC specimens; however, oak and spruce HMC specimens have higher IBS than LMC ones. Figure 17 also demonstrates that beech requires the highest amount of work, whilst spruce has the least IBS. Figure 18 compares the IBS for different orientations of each group.

Figures 19 and 20 show the boxplot of the max longitudinal strain of all groups. Based on Fig. 19, it can be realised that for all of the species, an increase in MC causes a clear increase in longitudinal strain in the centre of the lower region of the beam (9% for beech and 19% for oak and 18% for spruce). Also for both LMC and HMC groups, beech, oak and spruce have the highest to the lowest level of the max longitudinal strain up to crack initiation.

4 Conclusion

There were no statistical differences between radial and tangential directions for the maximum force, maximum strain, and work required for crack initiation of beech

and spruce wood. Thus the wood can be assumed to be transversally isotropic for impact loading. However, this assumption may not be correct for oak wood.

Moisture content significantly affects the maximum force, work required for crack initiation, deflection, max strain, and IBS. Max deflection and longitudinal strain increase by a rise in MC. While max force tends to decrease with MC elevation. For IBS, beech behaves unlike oak and spruce. IBS of HMC beech is less than LMC while the HMC groups of oak and spruce are higher than LMC.

The generalized force–time curves allowed us to identify five steps of the impact behaviour concerning the moisture content level. They can be used for experimental verification when the impact behaviour of wood will be modelled in different methods such as finite element method.

Author contribution All authors have accepted responsibility for the entire content of this manuscript and approved its submission.

Funding Open access publishing supported by the National Technical Library in Prague. This work was supported by the Ministry of Education Youth and Sports in the Czech Republic [Grant Number #LL1909, ERC CZ].

Availability of data and materials The data used in this study is available from the corresponding author on reasonable request.

Declarations

Conflict of interest Not applicable.

Ethical approval Not applicable.

Open Access This article is licensed under a Creative Commons Attribution 4.0 International License, which permits use, sharing, adaptation, distribution and reproduction in any medium or format, as long as you give appropriate credit to the original author(s) and the source, provide a link to the Creative Commons licence, and indicate if changes were made. The images or other third party material in this article are included in the article's Creative Commons licence, unless indicated otherwise in a credit line to the material. If material is not included in the article's Creative Commons licence and your intended use is not permitted by statutory regulation or exceeds the permitted use, you will need to obtain permission directly from the copyright holder. To view a copy of this licence, visit <http://creativecommons.org/licenses/by/4.0/>.

References

- Baumann G, Brandner R, Müller U, Stadlmann A, Feist F (2021) A comparative study on the temperature effect of solid birch wood and solid beech wood under impact loading. *Materials* 14(24):7616. <https://doi.org/10.3390/ma14247616>
- Bocchio, N., Ronca, P., Van De Kuilen, J.W. (2001). Impact loading tests on timber beams. In IABSE Conference: Innovative Wooden Structures and Bridges (pp. 29–31).
- Borůvka V, Zeidler A, Holeček T, Dudík R (2018) Elastic and strength properties of heat-treated beech and birch wood. *Forests* 9(4):197
- Cantwell WJ, Morton J (1991) The impact resistance of composite materials—a review. *Composites* 22(5):347–362
- ČSN 490115 (1979) Wood. Detection of static bending strength, Czech Standards Institute, Prague, Czech Republic
- ČSN 490117 (1980). Wood. Impact strength in bending, Czech Standards Institute, Prague, Czech Republic.
- Daniel IM, Gdoutos EE, Wang KA, Abot JL (2002) Failure modes of composite sandwich beams. *Int J Damage Mech* 11(4):309–334
- Dave MJ, Pandya TS, Stoddard D, Street J (2018) Dynamic characterization of biocomposites under high strain rate compression loading with split Hopkinson pressure bar and digital image correlation technique. *Int Wood Prod J* 9(3):115–121. <https://doi.org/10.1080/20426445.2018.1482673>
- Evcı C, Gülgeç M (2012) An experimental investigation on the impact response of composite materials. *Int J Impact Eng* 43:40–51. <https://doi.org/10.1016/j.ijimpeng.2011.11.009>
- Fortin-Smith J, Sherwood J, Drane P, Kretschmann D (2016) Characterization of maple and ash material properties as a function of wood density for bat/ball impact modeling in LS-DYNA. *Proced Eng* 147:413–418. <https://doi.org/10.1016/j.proeng.2016.06.331>
- Found MS, Howard IC, Paran AP (1998) Interpretation of signals from dropweight impact tests. *Compos Struct* 42(4):353–363
- Gaff M, Kačík F, Sandberg D et al (2019) The effect of chemical changes during thermal modification of European oak and Norway spruce on elasticity properties. *Compos Struct* 220:529–538
- Glass, S.V., Cai, Z., Wiedenhoef, A.C., et al (2010) Centennial Edition, *Wood Handbook—Wood as an Engineering Material*.
- Gómez A, Sanchez-Saez S, Barbero E (2021) Compression impact behaviour of agglomerated cork at intermediate strain rates. *Eur J Wood Prod* 79(2):381–396. <https://doi.org/10.1007/s00107-020-01638-2>
- Guo WG, Li YL, Liu YY (1997) Analytical and experimental determination of dynamic impact stress intensity factor for 40 Cr steel. *Theoret Appl Fract Mech* 26(1):29–34. [https://doi.org/10.1016/S0167-8442\(96\)00031-6](https://doi.org/10.1016/S0167-8442(96)00031-6)
- Haldar S, Gheewala N, Grande-Allen KJ, Sutton MA, Bruck HA (2011) Multi-scale mechanical characterization of palmetto wood using digital image correlation to develop a template for biologically-inspired polymer composites. *Exp Mech* 51(4):575–589
- Hao SW, Xia MF, Ke FJ, Bai YL (2010) Evolution of localized damage zone in heterogeneous media. *Int J Damage Mech* 19(7):787–804
- Hernández RE, Passarini L, Koubaa A (2014) Effects of temperature and moisture content on selected wood mechanical properties involved in the chipping process. *Wood Sci Technol* 48(6):1281–1301
- Jacques E, Lloyd A, Braimah A et al (2014) Influence of high strain-rates on the dynamic flexural material properties of spruce-pine-fir wood studs. *Can J Civ Eng* 41(1):56–64. <https://doi.org/10.1139/cjce-2013-0141>
- Jansson, B. (1992). Impact Loading of Timber Beams. Doctoral dissertation, University of British Columbia.
- Jiang F, Rohatgi A, Vecchio KS, Cheney JL (2004) Analysis of the dynamic responses for a pre-cracked three-point bend specimen. *Int J Fract* 127(2):147–165. <https://doi.org/10.1023/b:frac.0000035058.03627.30>
- Kalthoff JF (1985) On the measurement of dynamic fracture toughnesses—a review of recent work. *Int J Fract* 27(3–4):277–298. <https://doi.org/10.1007/BF00017973>
- Kubojima Y, Okano T, Ohta M (2000) Bending strength and toughness of heat-treated wood. *J Wood Sci* 46:8–15
- Lokaj A, Vavrušová K (2010) Wood impact bending strength laboratory tests. *Civ Eng Ser* 10(1):1–6
- Marsavina L, Sadowski T, Kneć M, Negru R (2010) Non-linear behaviour of foams under static and impact three point bending. *Int J Non-Linear Mech* 45(10):969–975. <https://doi.org/10.1016/j.ijnonlinmec.2010.03.007>
- Marur PR, Simha KRY, Nair PS (1994) Dynamic analysis of three point bend specimens under impact. *Int J Fract* 68(3):261–273. <https://doi.org/10.1007/BF00013071>
- Olmedo I, Bourrier F, Bertrand, et al (2015) Experimental analysis of the response of fresh wood stems subjected to localized impact loading. *Wood Sci Technol* 49(3):623–646. <https://doi.org/10.1007/s00226-015-0713-0>
- Pan B, Qian K, Xie H, Asundi A (2009) Two-dimensional digital image correlation for in-plane displacement and strain measurement: a review. *Meas Sci Technol* 20(6):062001. <https://doi.org/10.1088/0957-0233/20/6/062001>
- Polocoşer T, Stöckel F, Kasal B (2016) Low-velocity transverse impact of small, clear spruce and pine specimens with additional energy absorbing treatments. *J Mater Civ Eng* 28(8):04016048. [https://doi.org/10.1061/\(asce\)mt.1943-5533.0001545](https://doi.org/10.1061/(asce)mt.1943-5533.0001545)
- Polocoşer T, Kasal B, Stöckel F, Li X (2018) Dynamic material properties of wood subjected to low-velocity impact. *Mater Struct*. <https://doi.org/10.1617/s11527-018-1186-z>
- Rubio L, Fernández-Sáez J, Navarro C (2003) Determination of dynamic fracture-initiation toughness using three-point bending tests in a modified Hopkinson pressure bar. *Exp Mech* 43(4):379–386. <https://doi.org/10.1007/bf02411342>
- Thuvander F, Sjö Dahl M, Berglund LA (2000) Measurements of crack tip strain field in wood at the scale of growth rings. *J Mater Sci* 35(24):6267–6275. <https://doi.org/10.1023/A:1026722521248>
- Timbolmas C, Rescalvo FJ, Portela M, Bravo R (2022) Analysis of poplar timber finger joints by means of Digital Image Correlation (DIC) and finite element simulation subjected to tension

- loading. *Eur J Wood Prod* 80(3):555–567. <https://doi.org/10.1007/s00107-022-01806-6>
- Widmann R., Steiger R. (2009) Impact loaded structural timber elements made from Swiss grown Norway spruce. In *Proceedings of CIB-W18 Meeting* (Vol. 42), August.
- Wood LW. (1951). *Relation of strength of wood to duration of load* (No. 1916). US Department of Agriculture, Forest Service, Forest Products Laboratory.
- Xing MZ, Wang YG, Jiang ZX (2013) Dynamic fracture behaviors of selected aluminum alloys under three-point bending. *Def Technol* 9(4):193–200. <https://doi.org/10.1016/j.dt.2013.11.002>
- Yamada H, Tateyama K, Sasaki H et al (2018) Impact resistance to ballistic ejecta of wooden buildings and a simple reinforcement method using aramid fabric. *J Volcanol Geoth Res* 359:37–46. <https://doi.org/10.1016/j.jvolgeores.2018.06.014>
- Yokoyama T, Kishida K (1989) A novel impact three-point bend test method for determining dynamic fracture-initiation toughness. *Exp Mech* 29(2):188–194. <https://doi.org/10.1007/BF02321374>
- Yu JL, Jones N (1997) Numerical simulation of impact loaded steel beams and the failure criteria. *Int J Solids Struct* 34(30):3977–4004. [https://doi.org/10.1016/S0020-7683\(96\)00228-4](https://doi.org/10.1016/S0020-7683(96)00228-4)
- Zhang DS, Arola DD (2004) Applications of digital image correlation to biological tissues. *J Biomed Opt* 9(4):691–699

Publisher's Note Springer Nature remains neutral with regard to jurisdictional claims in published maps and institutional affiliations.